Japan Society of Civil Engineers
Yotsuya 1, Shinjuku-ku, Tokyo 160-0004
http://www.jsce.or.jp/

1. Source Characteristics and Strong Ground Motion

The January 13, 2001 Off the Coast of El Salvador Earthquake

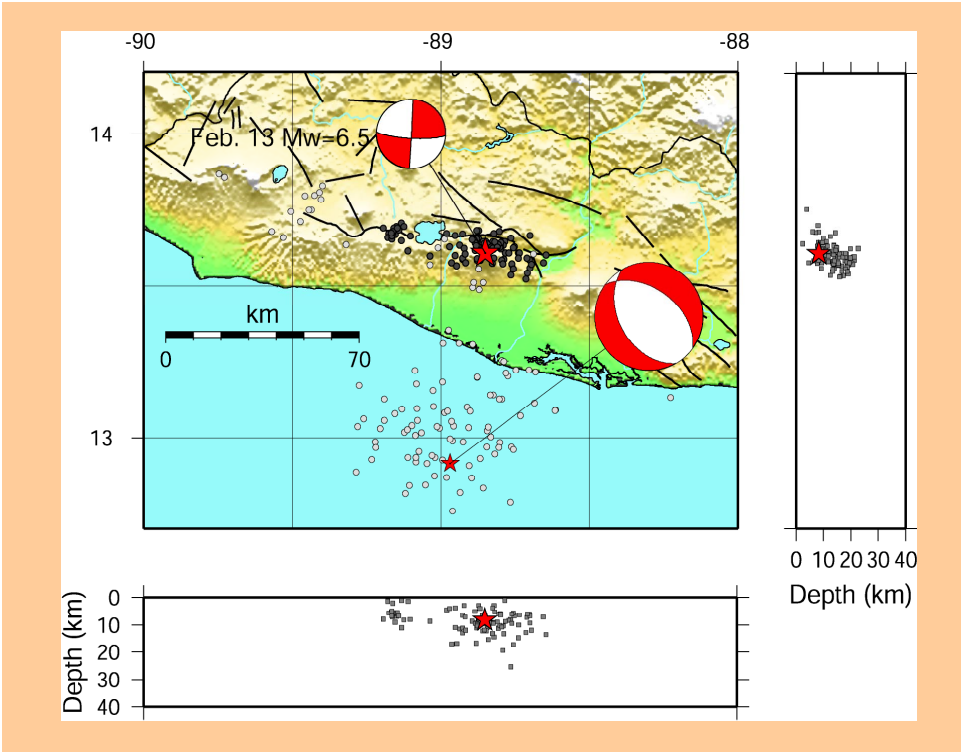

Aftershocks distributions of both Jan 13 and Feb 13 earthquakes

1.1 TECTONIC SETTING OF CENTRAL AMERICA AND THE 2001 El SALVADOR EARTHQUAKE

Tectonic setting of Central America and Recent Historical Earthquakes

The Central America tectonics is characterized by the interaction between the Caribbean and Cocos plates. The Cocos plate is subducting from the South-West towards the North-East beneath the Caribbean plate from the Middle American Trench at a relatively high rate (92 mm/year) with a steep subducting angle as can be seen in **Figure 1.1**.

El Salvador is located on the Pacific Ocean side of Central America. The country is crossed from west to east by a chain of quaternary volcanoes, the result of the subduction process. Two types of earthquakes can be characterized in the region; the ones within the volcanic range which are crustal earthquakes. This type of earthquakes despite having a magnitude not larger than approximately 6.5 have been historically responsible for the largest loss of life and damage in El Salvador as can be observed from **Table 1.1**. They have been mostly produced by right-lateral faults running parallel to the volcanic range as a result of the oblique convergence of the Cocos plate relative to the Caribbean plate. An example of this type of earthquake was the February 13, 2001 earthquake which was the largest "aftershock" following the El Salvador 2001 January 13 mainshock. The earthquakes of the second type are the subduction earthquakes occurring in the shear zone of the subducting Cocos plate and also within the plates. These earthquakes in the Central American subduction region have reached magnitudes larger than 8. The January 13, 2001 El Salvador mainshock is an example of this second type of earthquakes.

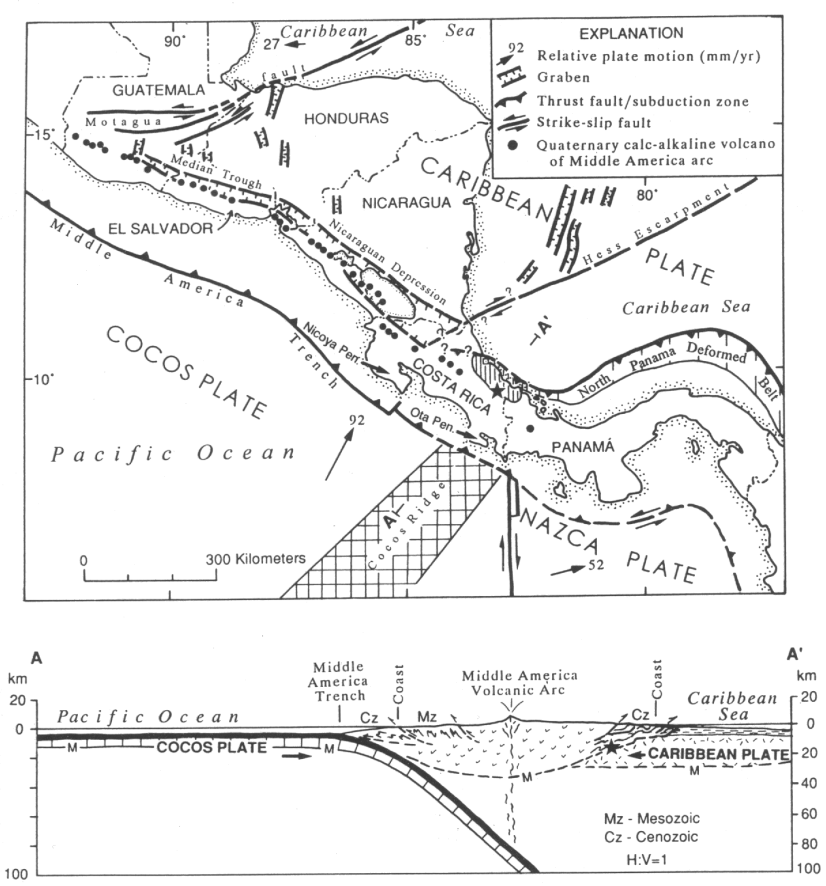

Figure 1.1. Tectonic Setting of Central America. The cross section of the subducting Cocos plate is shown (Plafker and Ward 1992).

Table 1.1. Source Parameters of recent destructive earthquakes in El Salvador (adapted from the CIG homepage)

Date	Lon. (W)	Lat. (N)	Magnitude	Depth	Type	Maximum Intensity (MM)	Damage	Ref.
6/5/1951	88.40	13.52	Ms=6.2 (White)	10	Crustal	-	400 dead	White (1993)
3/5/1965	89.15	13.65	Ms=6.0 (White)	10	Crustal	VII (San Salvador)	125 dead, 400 injured, 4000 collapsed houses	Lomnitz and Shulz (1966) White (1987)
19/6/1982	89.63	13.35	ML=7.0	80	Subduc-tion	VII (San Salvador)	8 dead, 96 injured	CIG (1983)
10/10/1986	89.19	13.67	Mb=5.4 (CIG-USGS)	8	Crustal	VIII-IX (San Salvador)	1500 dead, 10000 injured, 60000 collapsed houses	CIG
13/1/2001	88.968	12.915	Mw=7.6 (USGS)	32.1	Subduc-tion	VII (San Salvador)	944 dead (193 buried), 5565 injured, 108226 collapsed houses (COEN)	CIG
13/2/2001	88.851	13.608	Mw=6.5 (USGS)	8.2	Crustal	VI (San Salvador)	315 dead, 3399 injured, 41302 collapsed houses (COEN)	CIG

CIG : Centro de Investigaciones Geotécnicas (El Salvador)
COEN: Comité de Emergencia Nacional (El Salvador)
USGS: United States Geological Survey

The January 13 mainshock

The January 13 /2001 earthquake (Mw 7.6) was produced by the subduction of the Cocos plate beneath the Central American plate. The epicenter was located at approximately 50 km south of the coast of El Salvador at a depth of 32 km (Centro de Investigaciones Geotécnicas CIG). The solution of the focal mechanism determined by several agencies shows a normal fault, related with an extensional stress regime. The source parameters are summarized in **Table 1.2.**

The aftershocks distribution of the mainshock determined by the CIG National Seismic Network are distributed across an area of approximately 70 km along the strike and focal depths between 20 and 80 km (**Figure 1.2**). In the lower part of **Figure 1.2** we show a projection of the aftershocks (N36E) perpendicular to the USGS fault plane solution No2. We can clearly observe the range of focal depths above mentioned, but the aftershock distribution does not clearly show a particular fault plane.

Table 1.2. Source Parameters of the January 13, 2001 El Salvador earthquake

Agency	Strike,Dip,Rake Fault Plane No1	Strike,Dip,Rake Fault Plane No2	Mw	Lat. (W)	Lon. (N)	Depth (Km)
USGS	149, 45,-73	306,48,-107	7.6	12.767	88.827	39.0
Harvard-CMT	119,34,-98	309,56,-85	7.7	12.940	89.080	57.4
ERI	152,33,-78	318,58,-98	7.6	12.800	88.800	50.0

Harvard-CMT: Harvard University, Centroid Moment Tensor Solution
ERI: Earthquake Research Institute (Tokyo University)

From an analysis of the three different solutions of focal mechanisms in **Table 1.2**, we can observe that the actual fault plane that ruptured during the January 13 main shock has two main possibilities: one is a fault plane dipping to the south-west at a strike angle between 119° to 152° and a dip angle between 33° to 45°. The second possibility is a fault plane dipping to the northeast at a strike angle between 306° to 318° and a steeper dip angle between 48° and 58°.

In order to determine which was the actual fault plane that ruptured during the January 13/2001 earthquake it is necessary to perform a detailed study of the source rupture process by using all the available information of local strong motion recordings. Despite that such a study is beyond the scope of this survey report, in the coming sections we will try to examine which of the fault planes ruptured during the January 13, 2001 El Salvador earthquake by making a broadband frequency strong ground motion simulation of the available strong motion data.

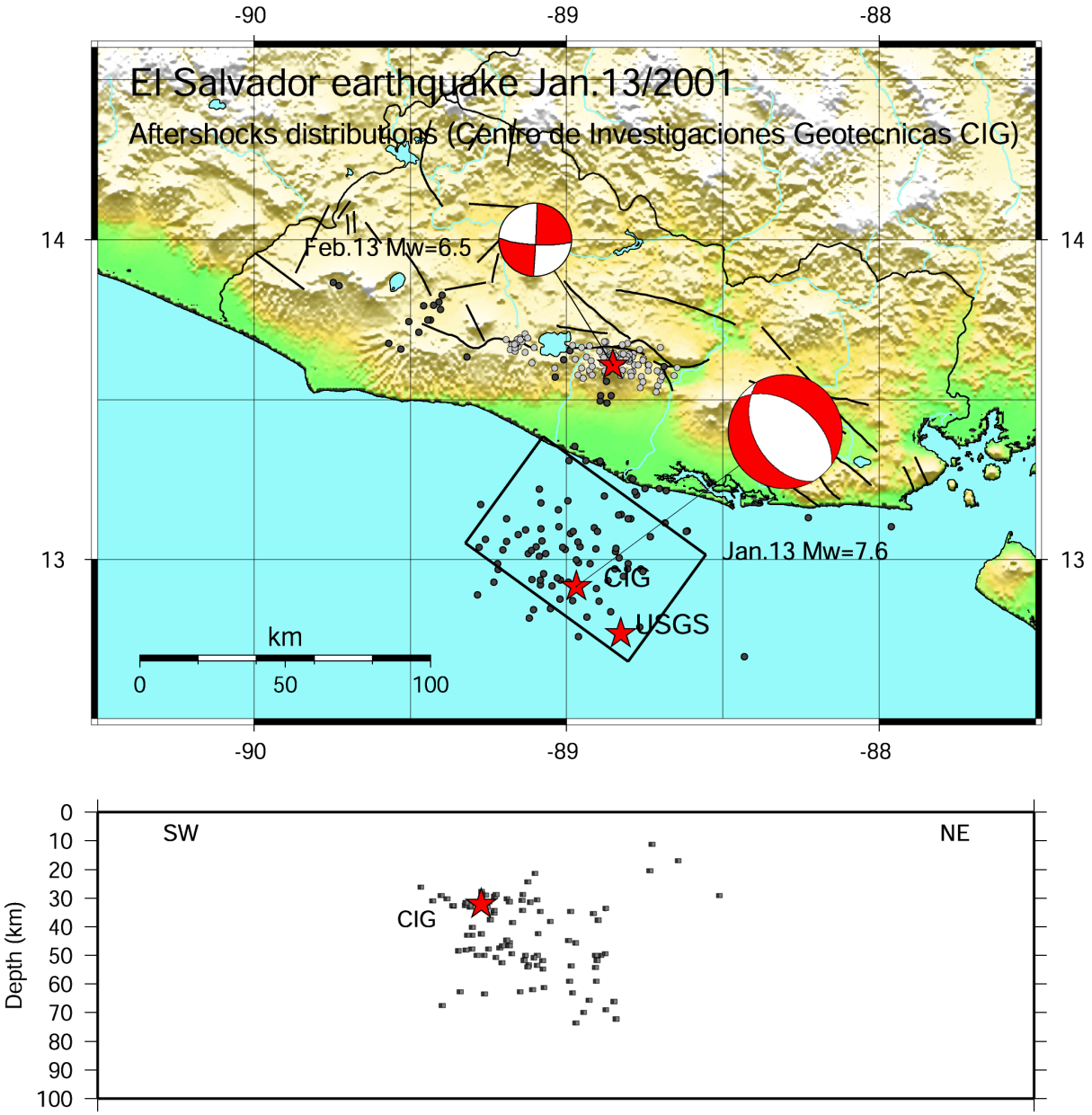

Figure 1.2. USGS focal mechanism solutions and CIG afterschocks distribution of the El Salvador January 13, 2001 earthquake (dark gray) and February 13, 2001 earthquake (light gray). The approximate rupture area corresponding to the USGS fault plane solution No2 is shown by a rectangle. The epicenter determined by CIG and USGS are shown by a star. The faults within El Salvador volcanic range are shown. Aftershocks projection of the January 13, 2001 earthquake, perpendicular to the USGS fault plane solution No2 is shown (Lower panel).

The February 13 aftershock

One month after the January 13 main shock a large earthquake (Mw 6.5, USGS) occurred in February 13/2001, with the hypocenter located 30 km east of San Salvador city at a depth of 8 km (CIG). This earthquake was a shallow strike-slip right-lateral event. Even though this earthquake did not happen in the epicentral region of the January 13 main shock, it is most probably related to complex stress changes in the active faults within the El Salvador volcanic range triggered by the January 13 earthquake. The aftershocks distribution of the February 13 earthquake determined by the CIG

National Seismic Network, clearly show a fault plane of about 30 km in length oriented from east to west, with focal depths from 25 km to the surface. **Figure 1.3** shows the aftershock distribution of the February 13 earthquake by including two aftershock projections to the South and to the East. The relative location of the epicenter respect to the aftershocks indicates that the earthquake was characterized by a bi-lateral rupture propagation.

The final slip distribution of the February 13 earthquake, from the inversion of teleseismic body-waves (Kikuchi and Yamanaka) shows a fault plane with an area of 30 km by 20 km with two asperities: a large asperity is located from the west side of the hypocenter and a smaller asperity located in the east side of the fault (**Figure 1.4**).

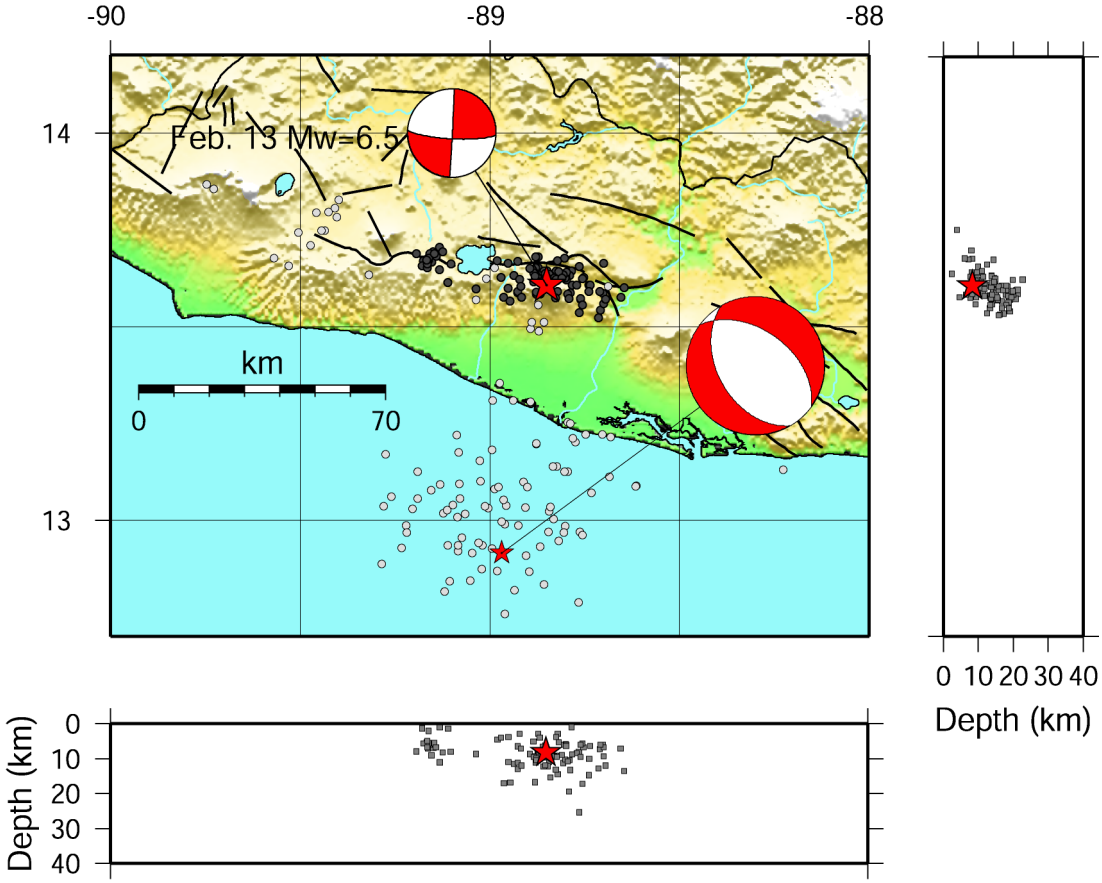

Figure 1.3. CIG afterschocks distribution of the February 13, 2001 El Salvador earthquake (dark gray). Aftershocks projection of the February 13 earthquake to the east (right panel) and to the south (lower panel). The aftershocks distribution of the January 13, 2001 earthquake is shown by a light gray.

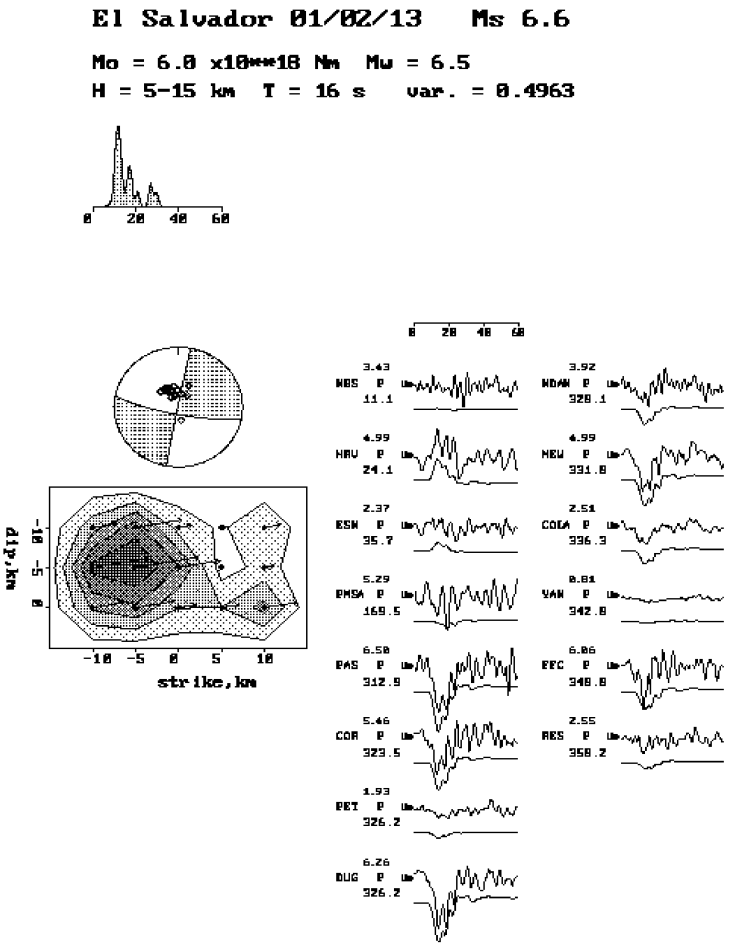

Figure 1.4. Source Inversion of the teleseismic body-waves (IRIS-DMC) of the February 13, 2001 earthquake at El Salvador (Kikuchi and Yamanaka).

1.2 STRONG GROUND MOTION CHARACTERISTICS

El Salvador seismic and strong motion networks

The El Salvador National Seismic Network is operated by the "Centro de Investigaciones Geotécnicas" (CIG). It consists of 13 telemetered short period vertical component stations located countrywide with the headquarters at San Salvador city (**Figure 1.5**).

Another seismic network is operated by the "Geotérmica Salvadoreña" (GeSal). That seismic network is located around the Berlin city for basically monitoring the local seismic activity around the Berlin Geothermal plant. The recorded seismic signals are also sent to the CIG headquarters.

The El Salvador National Strong Motion Network is operated by the CIG. The Strong Motion Network is composed by 21 stations including 5 open borehole stations with depths up to 30 mts in San Salvador city. Most of the instruments are of analog type Kinemetrics SMA-1. A second network of 10 digital accelerographs (Kinemetrics SSA-2) is operated by the "Universidad Centroamericana José Simeon Cañas" (UCA University). The network covers basically a region about 40 km around San Salvador city (Bommer et al. 1997). Additionally two digital accelerographs (SSA-2) are operated at the Berlin Geothermal Plant by the "Geotérmica Salvadoreña". The location of all the instruments can be observed in **Figure 1.5**.

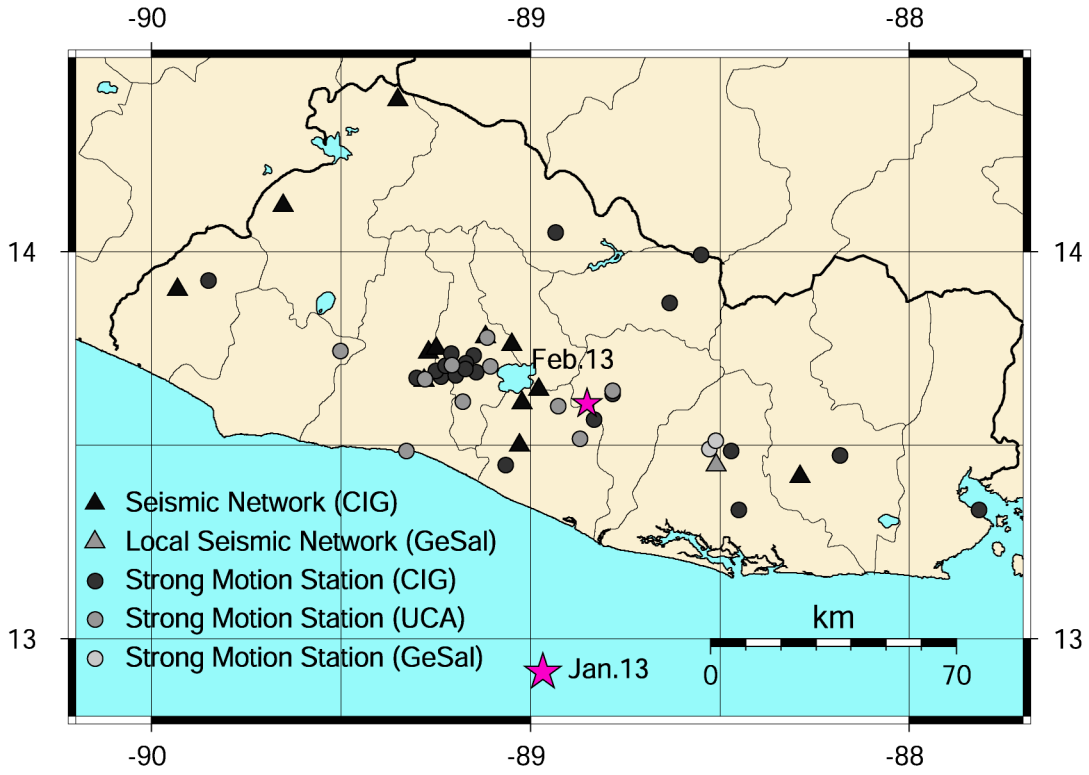

Figure 1.5. Location of the Seismic Networks and strong motion stations at El Salvador

Observed Ground motion distribution from the January 13 earthquake

The available strong ground motion recordings during the 2001 El Salvador earthquake (UCA 2001) show in general larger amplitudes in the western part of the country compared with the eastern part. This behavior can be observed in the recorded velocity waveforms shown in **Figure 1.6.** The largest PGV was obtained at the Santa Tecla Station (Te) with a value of approximately 57 cm/s (**Figure 1.6**). This ground motion was large enough to trigger the big landslide at Las Colinas. It must be said that the Te recording is located approximately 1 km away from Las Colinas site.

The acceleration waveforms show a similar behavior as can be appreciated from figure 2.7. The largest PGA (1109 cm/s^2) was recorded at La Libertad station (Li), (**Figure 1.7**).

The complexity of the velocity waveforms reveals a very complex velocity structure model. We can however appreciate from one of the closest stations to the fault plane (Li station) a 10 sec low frequency pulse probably associated with a forward rupture directivity of a large asperity (**Figure 1.6**). We can also see as a general observation that the NS components are larger in amplitude that the EW components.

All the waveforms shown in **Figure 1.5** and **1.6** have been recorded by the UCA strong motion network and also the GeSal instruments. The coverage of these stations is mostly around the San Salvador city area. The recordings from the CIG strong motion network were not available by the time of this survey report. The CIG strong motion information will help in the future to give a better idea about the strong ground motion distribution across the country.

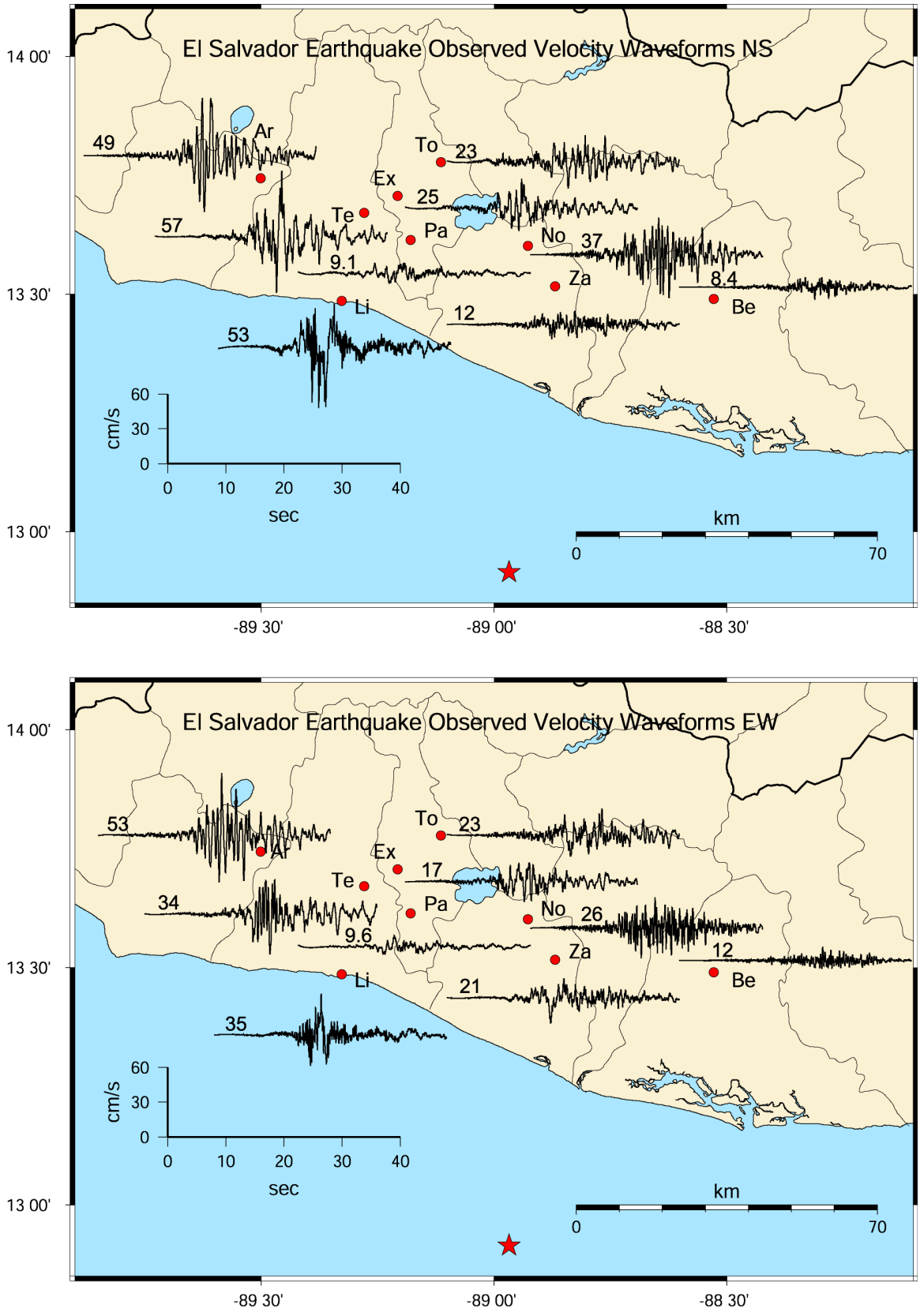

Figure 1.6. Spatial Distribution of the recorded velocities waveforms EW and NS components, during the January 13/2001 El Salvador earthquake. The PGV values at each station are shown. The CIG epicenter is shown by a star.

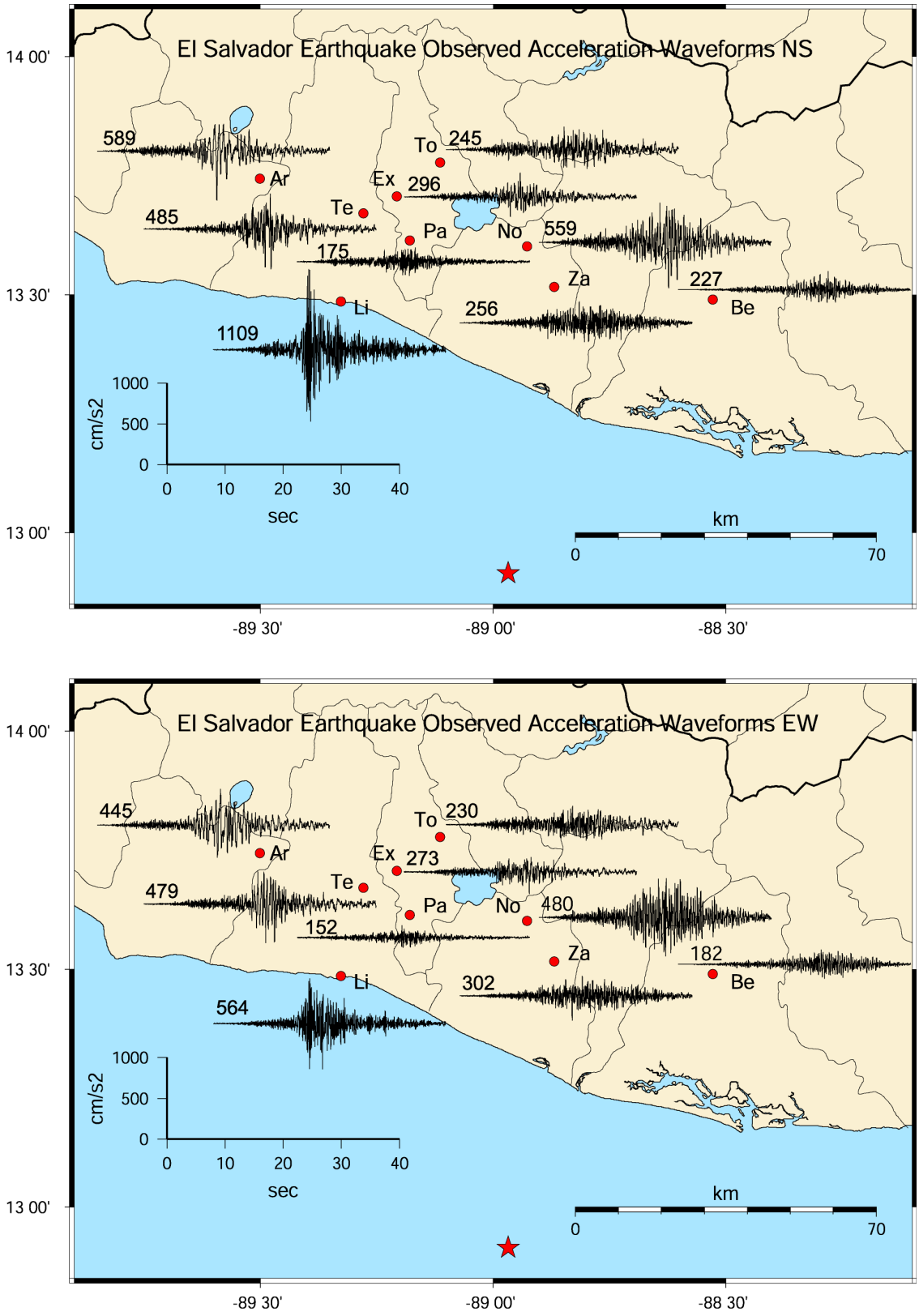

Figure 1.7. Spatial Distribution of the recorded acceleration waveforms EW and NS components, during the January 13/2001 El Salvador earthquake. The PGA values at each station are shown. The CIG epicenter is shown by a star.

1.3 BROADBAND STRONG GROUND MOTION SIMULATION OF THA JANUARY 13 EARTHQUAKE

Ground Motion Estimation Methodology

The basic idea of the simulation methodology is to evaluate the strong ground motion radiated from a finite source model composed of **asperities** or regions in the fault plane with a large slip, embedded in a layered velocity structure. The ground motion at a particular target station is obtained from the contribution of the radiation of all the asperities in the fault plane that are assumed to have a finite area. The ground motion estimation methodology aims to produce ground motions in a broadband frequency range (0.1Hz to 10 Hz) in order to be able to compare the simulated ground motions with the observed damage distribution.

The procedure to be applied is a hybrid ground motion simulation technique, which consists in the generation of ground motions in a low frequency (<1Hz) and high frequency (>1Hz) bands as illustrated in **Figure 1.8** (Kamae and Irikura 1998).

The low frequency part of the ground motion is calculated from the 3D radiation of an asperity model, propagating in a flat-layered velocity structure. For this purpose a Discrete Wave Number method for a 3D elastic wave propagation in a layered media is applied (Bouchon 1981). An extended source discretized into several sub faults is used to calculate the ground motion from each asperity. The contribution from each sub fault inside the asperities is time delayed according to an assumed rupture velocity.

The high frequency motion generation uses the idea of the empirical Green's function technique (Irikura 1983), which consists in using recordings from small events (aftershocks) in order to reproduce the ground motion from a large event (main shock). For that purpose the scaling relation of the source spectra and the source parameters together with an appropriate selection of the small event is considered. For regions, where no appropriate recording of aftershocks is available, the seismograms of the small event are generated stochastically in such a way that they follow an omega square model and a regional attenuation relationship (Boore 1983). Then the empirical Green's function method is applied using the synthetic aftershock waveform obtained previously.

Finally the amplification of the seismic waves and the nonlinearity effect of surficial layers should be included to get the ground motion at a specific site. The final motion is obtained from the summation of the low and high frequency parts obtained before.

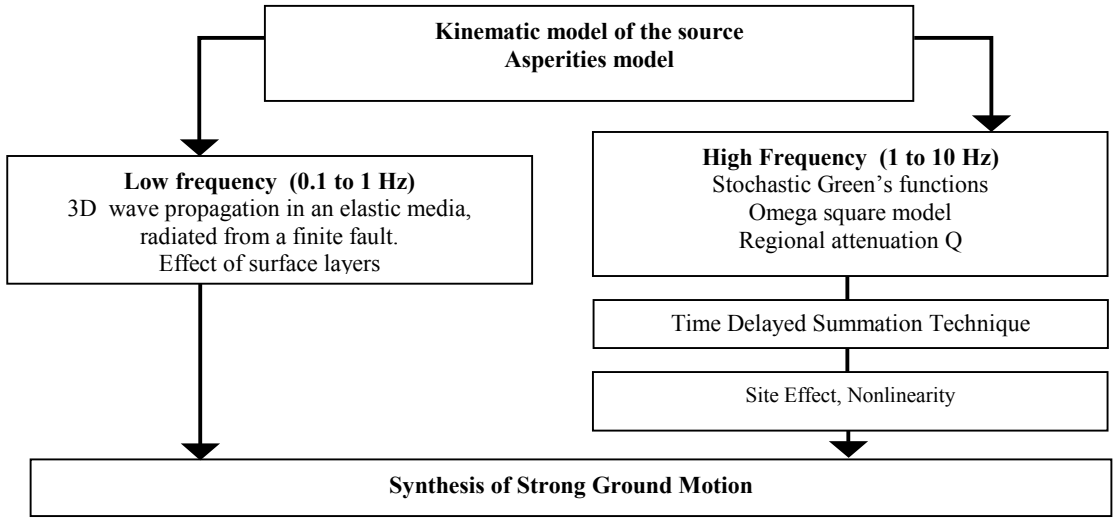

Figure 1.8. Broadband frequency strong ground motion simulation procedure.

High Frequency Ground Motion

The stochastic Green's functions are calculated according to Boore (1983). The waveforms are generated to meet an acceleration Fourier spectra that follows an omega square model and a regional attenuation relationship. We modified the original equation of Boore in order to include a frequency dependent site effect F(w) into the acceleration Fourier spectra as follows:

$$A(w) = f(R_{\theta\phi}) M_0 F(w) S(w, w_c) A_t(Q, w) \tag{1.1}$$

where: w is the frequency, A(w) is the acceleration Fourier spectra, $f(R_{\theta\phi})$ the radiation pattern, M_o Seismic Moment and $F(w)$ is a frequency dependent site effect.

The source omega square model is defined as follows:

$$S(w, w_c) = \frac{w^2}{1 + (\frac{w}{w_c})^2} \tag{1.2}$$

where w, w_c are frequency and corner frequency respectively.

The regional attenuation is calculated in the following way:

$$A_t(Q, w) = \frac{e^{-wR/2Q\beta}}{R} \tag{1.3}$$

where Q is the quality factor, R is the epicentral distance, β is the S wave velocity

The empirical Green's Function Method (Irikura 1986) is then use to calculate the ground motion from the same asperity model as in the low frequency case. Each asperity is discretized into several subfaults as in **Figure 2.1.6**, and the green function from them is calculated from the stochastic methodology above described. The total ground motion from the asperity is obtained by the convolution of the ground motion from each subfault u(t) with a scaling function between the slip of the large event and small event:

$$U(t) = \sum_{i=1}^{N} \sum_{j=1}^{N} \frac{r}{r_{ij}} F(t - t_{ij}) * u(t) \tag{1.4}$$

where: U(t) is the ground motion of main (target) event and u(t) is the ground motion small event.
The rupture delay time t_{ij}, slip scaling between the large and small event F(t) and scaling source parameter N are shown as follows:

$$t_{ij} = \frac{r_{ij} - r_0}{\beta} + \frac{\xi_{ij}}{V_r} \tag{1.5}$$

$$F(t) = \delta(t) + \frac{1}{n'} \sum_{k=1}^{(N-1)n'} \delta(t - (k-1)\frac{\tau}{(N-1)n'}) \tag{1.6}$$

$$N = (\frac{M_{0t}}{cM_{0s}})^{1/3} \tag{1.7}$$

where: r_o , r_{ij} are the distance between the target station and the hypocenter and ij subfault respectively (**Figure 2.9**), ξ_{ij} is the distance between the hypocenter and the ij subfault, β is the S wave velocity, τ is the rise time of the target event, 'n' is an integer to reduce spurious periodicity related with the summation procedure (Irikura 1983), Vr is the rupture velocity, M_{ot} and M_{os} are the target and small event seismic moments and c is the stress drop ratio between the large and small event.

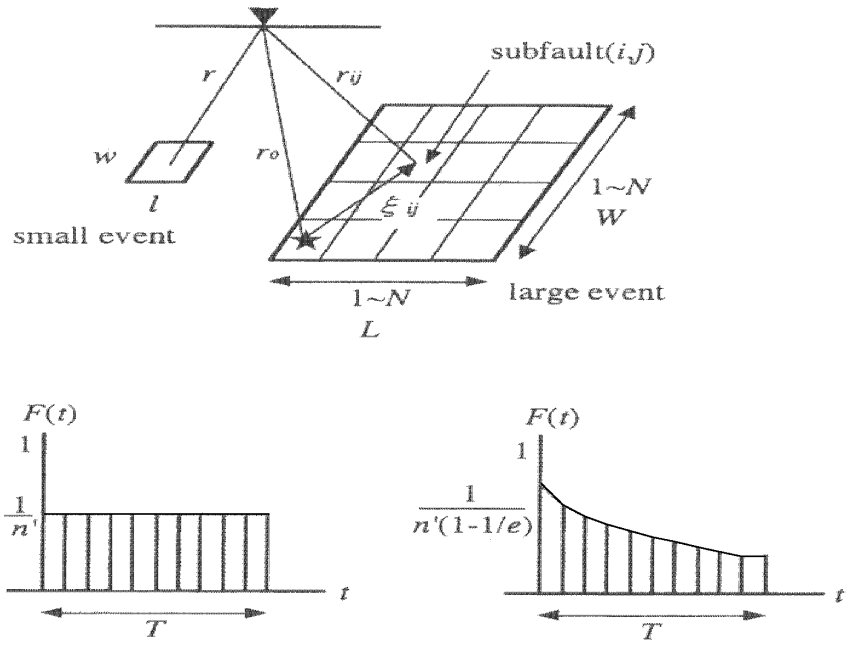

Figure 1.9 Empiricals Green's function. Fault discretization and sub fault summation (modified from Miyake et al. 1999).

Strong ground motion simulation of the January 13/2001 El Salvador earthquake

We performed a broadband frequency strong ground motion simulation of the January 13, 2001 El Salvador earthquake at the Santa Tecla (Te) and la Libertad (Li) stations as can be appreciated in **Figure 1.10**.

The first step of the simulation was determining which fault plane preferably ruptured during the El Salvador earthquake by selecting the solution that optimized the fitting of the velocity and acceleration waveforms as well as velocity and acceleration response spectra. For that purpose we analyzed the six possible fault plane solutions given in **Table 1.2**. As observed before those solutions can be basically divided into two groups: a fault plane dipping to the Northeast and a fault plane dipping to the Southwest. For Each solution we assumed a fault plane consisting of only one asperity whose seismic moment was assumed to be a 40% of the total seismic moment of the earthquake (USGS seismic moment) with no background slip in the fault plane (**Figure 1.10**). The asperity area was determined according to the empirical scaling between seismic moment and asperity area determined for the earthquake slip models available for California (Somerville et al. 1999).

We made first a forward modeling of the low frequency waveforms (0.1 to 1 Hz) at the Li and Te stations, for each of the six possible fault plane mechanism. In each case we also tried different locations of the asperity. We finally obtained among the set of possibilities analyzed that the solution giving the best fit to the waveforms was the one corresponding to the USGS fault plane solution No.2, namely a fault plane dipping to the North-East as can be seen from **Figure 1.10**. We found that a preferred location of the asperity is close to the hypocenter, that we assumed to be the one determined by the CIG El Salvador Seismic Network (**Table 1.1**).

The rise time and rupture velocity were also selected in order to optimize the fitting between the observed and simulated velocity waveforms. The parameters used for the simulation are summarized in **Table 1.3**. The crustal velocity structure model used for the computation of the low frequency Green's function (**Figure 1.11**) was adapted from a lithospheric structure model of the Costa Rican Isthmus (Sallares V., and Dañobeitia J.J. 2001).

Table 1.3. Characterized asperity model of the January 13, 2001 El Salvador earthquake

Rupture area (km^2)	70 x 70
Fault Mechanism (strike,dip,rake)	306,48,-107 (USGS)
Seismic moment (Nm)	3.2×10^{20} (USGS)
Number of asperities	1
Asperity area (km^2)	30 x 30
Seismic moment asperity (Nm)	1.28×10^{20}
Stress Drop (bar)	115
Asperity Rise Time (sec)	1.0
Rupture velocity outside asperity (km/sec)	3.5
Rupture velocity inside asperity (km/sec)	2.9
Starting Point of the rupture	Shown in figure 3.10
Number of subfaults inside asperity	36
Average S-wave velocity (km/sec)	3.99
Average density (kg/m^3)	2990
Frequency range of predicted ground motions	0.1 to 10.0 Hz

The second step of the simulation was the inclusion of the high frequency part into the waveforms (1 to 10 Hz). For performing this step we used the asperity model obtained from the low frequency part. The high frequency simulation was performed by using the empirical Green's function method described in **Section 1.3**. The element or subfault waveform was calculated using a stochastic approach (**Section 1.3**). The element waveform acceleration spectrum is composed by three main factors: source spectra, regional attenuation spectra and site effect. We assumed an omega-square source spectra and frequency dependent attenuation. The stress drop is calculated from the seismic moment and asperity area from a theoretical relationship.

A big concern of the simulation was the one related with the site effects. From the observed acceleration response spectra at the Li station for both the NS and EW components (**Figures 1.12** and **1.13**) we can observe a very large spectral acceleration peak at approximately 0.2 seconds. We think this peak is related with the site conditions at the Li station. In fact we found that the only way of enlarging the simulated acceleration spectra for periods between 0.1 and 1.0 sec to get closer to the observed acceleration spectra, was by means of applying the spectral site effect factor in Equation (1.1). For the Li station we found that a very large spectral factor of 7 is needed to get closer to the observed acceleration spectra in the short period range. This observation also holds for the maximum amplitude of the acceleration waveforms (**Figure 1.12** and **1.13**). On the other hand we observed that the velocity waveforms are less sensitive to the site effect, and are mostly dominated by the low frequency part as can be seen from **Figure 1.12** and **1.13**.

A similar observation holds for the Te station. From the observed acceleration spectra for both NS and EW components (**Figure 1.14** and **1.15**) we can see large values of spectral acceleration for periods between 0.2 and 0.6 seconds. Again in order to get a good fitting in this range of periods a spectral site effect factor of 5 should be applied. As for the previous case we found that the acceleration waveforms are more sensitive to the site effect compared with the velocity waveforms (**Figures 1.14** and **1.15**).

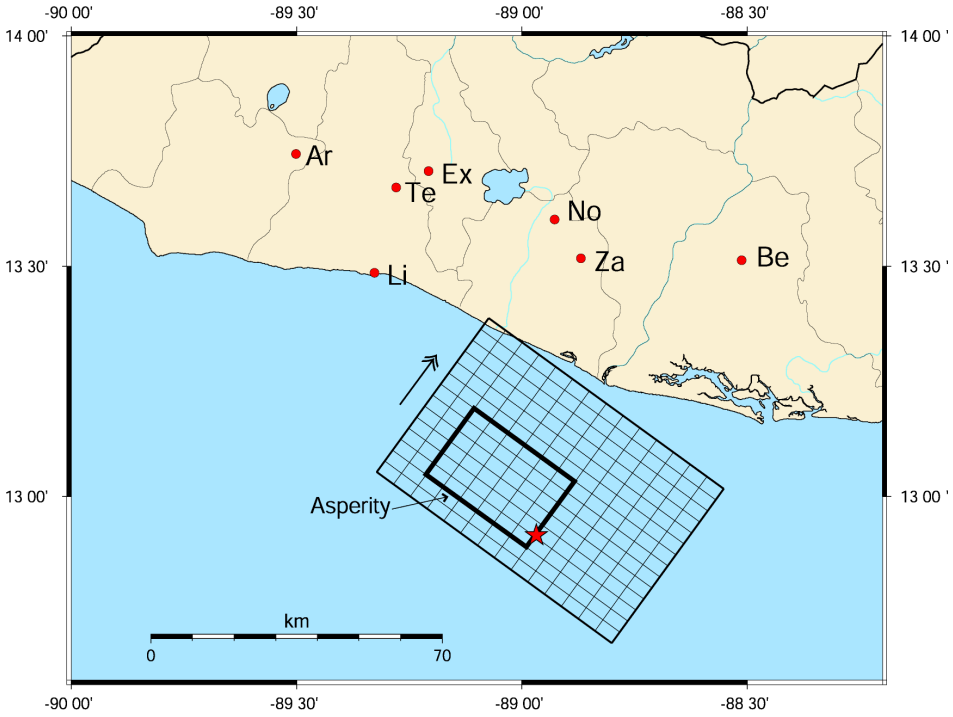

Figure 1.10 Asperity Model of the January 13, 2001 El Salvador earthquake. The fault plane corresponding to the USGS focal mechanism No. 2 is assumed (strike 306, dip 48, rake –107).

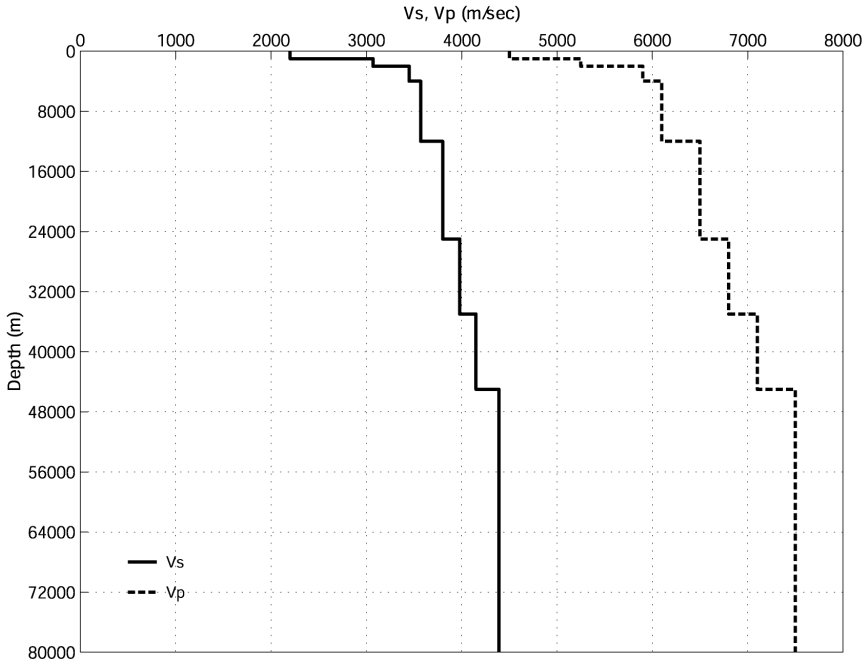

Figure 1.11 Crustal velocity structural model assumed for the broadband frequency simulation of the January 13, 2001 El Salvador earthquake (after Sallares V., and Dañobeitia J.J. 2001)

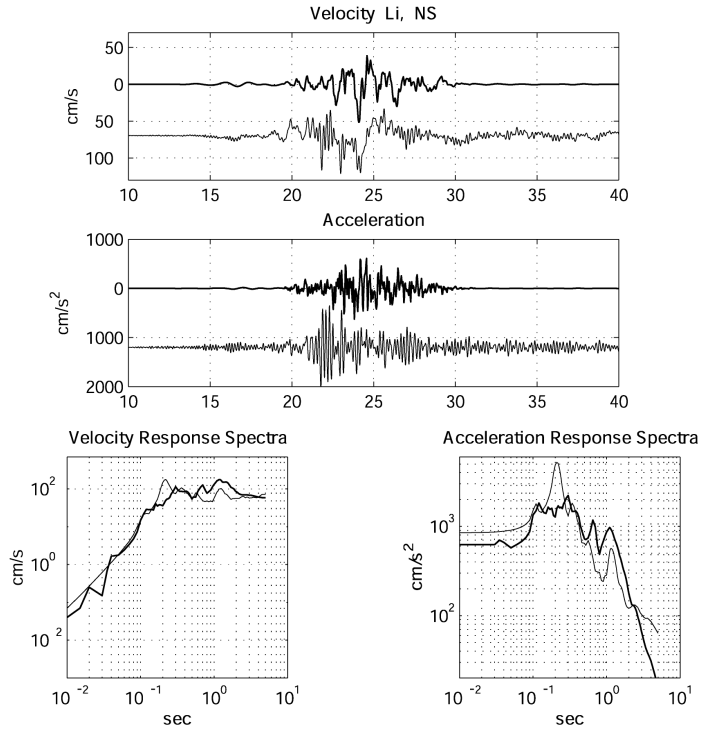

Figure 1.12 Comparison between the simulated (thick line) and observed NS component (velocity and acceleration waveforms and reponse spectra) at the Li station (Unidad de Salud, La Libertad) during the January 13, 2001 El Salvador earthquake. The waveforms are bandpassed filtered between 0.1 and 10 Hz.

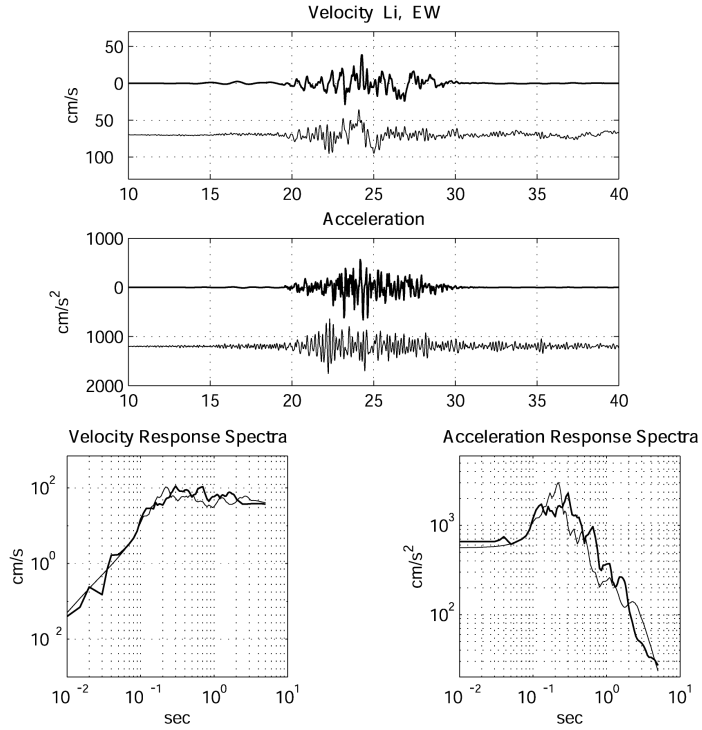

Figure 1.13. Comparison between the simulated (thick line) and observed EW component (velocity and acceleration waveforms and response spectra) at the Li station (Unidad de Salud, La Libertad) during the January 13, 2001 El Salvador earthquake. The waveforms are bandpassed filtered between 0.1 and 10 Hz.

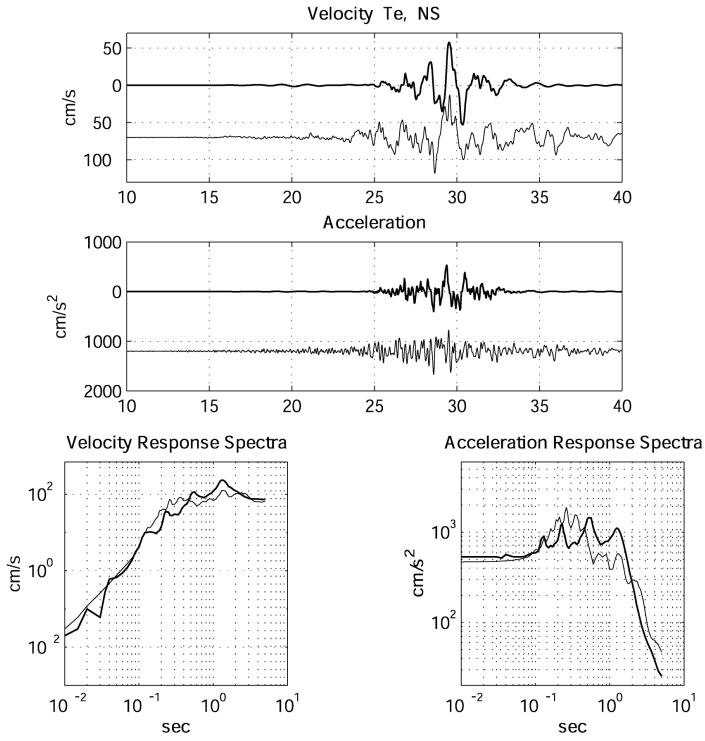

Figure 1.14. Comparison between the simulated (thick line) and observed NS component (velocity and acceleration waveforms and response spectra) at the Te station (Hospital San Rafael, Santa Tecla) during the January 13, 2001 El Salvador earthquake. The waveforms are bandpassed filtered between 0.1 and 10 Hz.

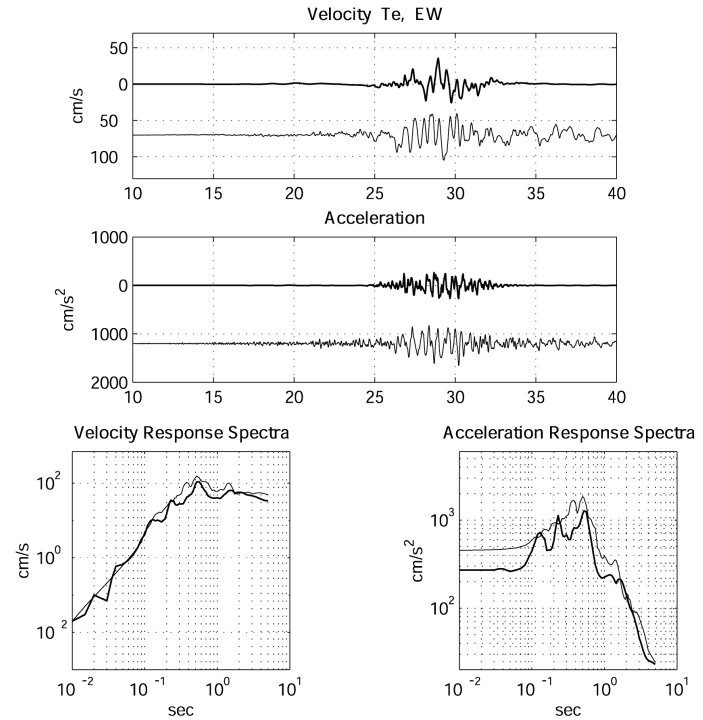

Figure 1.15 Comparison between the simulated (thick line) and observed EW component (velocity and acceleration waveforms and response spectra) at the Te station (Hospital San Rafael, Santa Tecla) during the January 13, 2001 El Salvador earthquake. The waveforms are bandpassed filtered between 0.1 and 10 Hz.

1.4 DISCUSSION AND CONCLUSIVE REMARKS

Several fault plane solutions were analyzed in order to understand which of the possible fault planes ruptured during the January 13, 2001 El Salvador earthquake. Among the set of possible solutions considered a fault plane dipping to the Northeast with an asperity rupturing from east to west, starting close to the epicentre was found to give an optimum spectral and waveform fitting at the Li and Te stations. However this rupture model is only given as a rough approximation of the rupture process of the earthquake, since the number of stations used and available are very limited and there is a large uncertainty about the actual fault plane that ruptured during the January 13, 2001 El Salvador earthquake. Another source of uncertainty is the one regarding to the crustal velocity model of El Salvador.

A more detailed source rupture model of the earthquake is required if more strong motion stations are available in a near future.

From the observed strong motion recordings we can observe that the waveforms tends to be larger towards the west (in particular the velocity waveforms). This could be related with a forward rupture directivity produced by the asperity found by our model, where the rupture propagates from east to west producing a forward directivity pulse clearly seen in the Li station.

We found that the site effect has a large influence in the short period range of the Li and Te stations. We optimised the spectral fitting between observations and simulations at this period range by including a large factor of spectral amplification into the simulations. Concerning the waveforms amplitudes we found that the acceleration waveforms are more sensitive to the site effect compared with the velocity waveforms.

There is an urgent need to enlarge both the El Salvador Seismic and Strong Motion Networks. The actual coverage of the country is poor especially in the Eastern part and along the coast.

There is also an urgent need to promote a study of the active faults of El Salvador in particular to determine the activity of the faults within the El Salvador volcanic range. It was made clear by the occurrence of the January 13, 2001 El Salvador earthquake the very complex relationship between the subduction earthquakes and the shallow crustal earthquakes. The January 13 mainshock most probably triggered the very active crustal seismicity around the San Salvador region, in particular the February 13, 2001 earthquake that left a large dead toll and damage comparable with that of the mainshock. It has been observed that historical crustal earthquakes have been responsible for the largest human losses and damage in El Salvador.

ACKNOWLEDGEMENT

We would like to express our gratitude to the Centro de Investigaciones Geotécnicas (CIG) for providing the aftershocks activity information. Also to Patricia Hasbun of the UCA University for providing the strong motion recordings used in this study. We also would like to sincerely thank to Salvador Handel and Jose A. Rivas of GeSal for all the information and support provided during our reconnaissance survey of El Salvador 2001 earthquake and also for providing the strong motion recording of the Berlin station.

REFERENCES

Boore, D. M., (1983). "Stochastic simulation of high frequency ground motions based on seismological models of the radiation spectra," *Bull. Seism. Soc. Am.*, **73**, 1865-1894.

Bommer J., A. Udias, J. Cepeda, J. Hasbun, W. Salazar, A. Suarez, N. Ambraseys, E. Buforn, J. Cortina, R. Madariaga, P Mendez, J. Mezcua, D. Papastamatiou, (1977). "A New Digital Network for El Salvador," *Seism. Res. Lett.*, **68(3)**, 426-437.

CIG (Centro de Investigaciones Geotécnicas,El Salvador). Historical Seismicity at El Salvador. (http://www.geotecnico.com/Sismologia/1crono.htm in Spanish)

CIG (Centro de Investigaciones Geotécnicas,El Salvador). El Salvador January 13/2001 earthquake and its aftershocks. (http://www.geotecnico.com/Sismologia/1sub.htm in Spanish)

CIG (Centro de Investigaciones Geotécnicas,El Salvador). El Salvador February 13/2001 earthquake and its aftershocks. (http://www.geotecnico.com/Sismologia/1sv.htm in Spanish)

COEN (Comité de Emergencia Nacional, El Salvador). Report on the El Salvador January 13/2001 and February 13/2001 disasters (http://www.coen.gob.sv in Spanish).

Earthquake Research Institute (ERI), Tokyo University, El Salvador January 13/2001 earthquake, (http://wwweic.eri.u-tokyo.ac.jp/topics/200101131733/ in Japanese)

Earthquake Research Institute (ERI), Tokyo University, El Salvador February 13/2001 earthquake, (http://wwweic.eri.u-tokyo.ac.jp/EIC/EIC_News/010213.html in Japanese)

Harvard University Seismology, Harvard Centroid Moment Tensor Catalogue, CMT Solutions (http://www.seismology.harvard.edu/CMTsearch.html).

Irikura, K., (1986). "Prediction of strong acceleration motion using empirical Green's function," *7th Japan. Earthq. Eng. Symp.* 151-156.

Lomnitz, C., R. Schulz, (1966). "The San Salvador Earthquake of May 3, 1965," *Bull. Seism. Soc. Am.* **56**, 561-575.

Kamae, K., K. Irikura, A. Pitarka, (1998). "A Technique for Simulating Strong Ground Motion Using Hybrid Green's Function," *Bull. Seism. Soc. Am.,* **88(2)**, 357-367.

Miyake, H., T. Iwata, and K. Irikura, (1999). "Strong ground motion simulation and source modeling of the Kagoshima-ken Hokuseibu earthquakes of March 26(MJMA6.5) and May 13(MJMA6.3),1997, using empirical Green's function method," *Zisin2*, **51**, 431-442 (In Japanese with English abstract).

Molnar P., R. Rykes, (1969). "The tectonics of the Caribbean and Middle America regions from focal mechanisms and seismicity," *Bull. Geol. Soc. Am.* **80(4)**, 1639-1684.

NEIC-USGS. Earthquake Bulletin, El Salvador January 13/2001 earthquake. (http://neic.usgs.gov/neis/bulletin/01_EVENTS/010113173329/010113173329.HTML)

NEIC-USGS. Earthquake Bulletin, El Salvador February 13/2001 earthquake. http://neic.usgs.gov/neis/bulletin/01_EVENTS/010213142205/010213142205.HTML

Plafker G., S. Ward (1992). "Backarc thrust faulting and tectonic uplift along the Caribbean Sea coast during the April 22, 1991 Costa Rica earthquake," Tectonics, **11**, 709-718.

Sallares V., and J.J. Dañobeitia (2001). "Lithospheric structure of the Costa Rican Isthmus: Effects of subduction zone magmatism on an oceanic plateau," *J. Geophys. Res.,***106(B1)**, 621-643.

Somerville, P., K. Irikura, R. Graves, S. Sawada, D. Wald, N. Abrahamson, Y. Iwasaki, T. Kagawa, N. Smith, A. Kowada, (1999). "Characterizing Crustal Earthquake Slip Models for the Prediction of Strong Ground Motion," *Seismological Research Letters.*, **70**, No.1, 59-80.

UCA (2001) Strong motion data from the January-February 2001 earthquakes in El Salvador. Universidad Centroamericana, San Salvador, El Salvador.

White R. et al. (1987). "The San Salvador Earthquake of October 10th, 1986 – Seismological Aspects and other Recent Local Seismicity," Earthquake Spectra, **3**.

White R., D. Harlow, (1993), Destructive upper crustal earthquakes in Central America since 1900, *Bull. Seism. Soc. Am.,* **83(4)**, 1115-1142.

to the next page